Dynamics of Ion Locking in Doubly Polymerized Ionic Liquids

Swati Arora, Julisa Rozon, and Jennifer E. Laaser*

Department of Chemistry, University of Pittsburgh, Pittsburgh, PA

E-mail: j.laaser@pitt.edu

Abstract

In this work, we investigate the dynamics of ion motion in "doubly-polymerized" ionic liquids (DPILs) in which both charged species of an ionic liquid are covalently linked to the same polymer chains. Broadband dielectric spectroscopy is used to characterize these materials over a broad frequency and temperature range, and their behavior is compared to that of conventional "singly-polymerized" ionic liquids (SPILs) in which only one of the charged species is attached to the polymer chains. Polymerization of the DPIL decreases the bulk ionic conductivity by four orders of magnitude relative to both SPILs. The timescales for local ionic rearrangement are similarly found to be approximately four orders of magnitude slower in the DPILs than in the SPILs, and the DPILs also have a lower static dielectric constant. These results suggest that copolymerization of the ionic monomers affects ion motion on both the bulk and the local scales, with ion pairs serving to form strong physical crosslinks between the polymer chains. This study provides quantitative insight into the energetics and timescales of ion motion that drive the phenomenon of "ion locking" currently under investigation for new classes of organic electronics.

Introduction

In the past decade, polymerized ionic liquids (PILs) have attracted significant interest as solid electrolytes due to their high chemical stabilities, broad electrochemical windows, and mechanical durability.[1–3] With one of the charged species of an ionic liquid covalently tethered to the polymer backbone while the other remains free to move, PILs function as single-ion conductors and allow efficient ion transport in mechanically-robust materials.[4–6] To date, PIL materials have found applications in battery separators,[7,8] electrolytes for batteries and flexible electronics,[9–11] and gate dielectrics for field-effect transistors,[12,13] to name only a few. Because these applications typically require high ionic conductivities, most work to date has focused on increasing ion mobility without degrading the mechanical properties of the material.[14–18]

Recently, however, Liang *et al.* demonstrated that dramatically *decreasing* the ion mobility in ion-containing polymers, in a way that effectively locks non-equilibrium ion distributions in place, may also be useful for new classes of organic electronics.[19,20] In this work, a "doubly-polymerizable" ionic liquid (DPIL), in which both the cationic and anionic species bore polymerizable groups, was deposited onto a graphene-based transistor and polymerized under an applied voltage. With an appropriate device configuration, accumulation of ions near the electrodes induced p-n junctions in the underlying semiconductor. By polymerizing the DPIL while in this state, it was possible to "lock" the ions in place, producing a stable p-n junction that persisted even after the programming voltages were turned off.[20] Because two-dimensional semiconductors are difficult to dope using conventional substitutional doping approaches,[21] formation of persistent doping patterns via ion locking offers exciting new avenues for thin, flexible electronics based on these types of substrates.

This application relies on a significant restriction of ion transport upon polymerization, and builds on similar phenomena observed in the small number of other doubly-polymerizable and polyampholyte ionic liquid systems studied to date.[22–25] In 2002, Yoshizawa *et al.* demonstrated that polymerization of ionic liquids composed of vinylimidazole and vinyl-

sulfonic acid led to a precipitous drop in conductivity, with conductivities on the order of 10^{-9} S/cm measured at room temperature.[22] The addition of a small amount of non-polymerizable LiTFSI increased the conductivity by 4-5 orders of magnitude, highlighting the critical role of free ions in the overall ion mobility in these materials.[22] Shaplov *et al.* similarly demonstrated a considerable drop in ionic conductivity upon removal of mobile counterions from copolymers of pyrrolidinium or imidazolium-based cationic monomers with sulfonate-based anionic monomers.[23] More recently, Gu *et al.* and Fouillet *et al.* investigated polyampholytic copolymers of protic ionic liquids. Gu *et al.* found that the proton conductivity of these materials was very low in the absence of added mobile ions (ca. 10^{-10} S/cm to room temperature), similar to results obtained in aprotic systems;[24] while Fouillet *et al.* did not directly investigate the ion transport properties of the resulting materials, the high moduli and glassy behavior of the materials suggested significantly reduced molecular-scale dynamics.[25] It is thus clear that the ionic conductivity of PILs is strongly affected by polymerization of both the ionic species. However, a significantly deeper molecular-scale understanding of the mechanisms of ion locking and ion relaxation in these materials will be critical for optimizing them for useful applications.

One promising technique for investigating the dynamics of ion motion in polymerized ionic liquids is broadband dielectric spectroscopy (BDS).[26] In this technique, an oscillating voltage is applied across two electrodes that form a parallel plate capacitor with the sample sandwiched between the electrodes. The measured frequency-dependent dielectric response directly reflects the timescales of dielectric relaxation in the material, which may arise from processes such as ion-transport, sidechain reorientation, and segmental motion of the polymer backbones.[27–30] Recently, broadband dielectric spectroscopy has successfully been used by a number of groups to unravel the charge transport mechanisms and glassy dynamics in imidazolium-based polymerized ionic liquids, revealing that ion hopping is critical to achieving rapid ion transport and high conductivities in these materials.[30–35] Investigation of polymerized ionic liquids with systematically-varied linkers between the ionic moiety and

the polymer backbone, pendant alkyl chains, and ionic groups have similarly identified a number of chemical features that affect ion conduction in these materials.[29,36–38] The dynamics of ion motion also appear to be strongly affected by the nanoscale structure of the materials, which can, depending on the polymer chemistry, separate into polar and nonpolar domains on the length scale of single monomers.[28,39,40] The successful application of BDS to this wide range of polymerized ionic liquid systems thus makes it an attractive technique for understanding the dynamics of ion motion in DPILs, as well.

Here, we exploit broadband dielectric spectroscopy to investigate and quantify the timescales of ion motion and polymer relaxation in a DPIL analogous to [EMIM][TFSI], and compare the dielectric behavior of the DPIL to the conventional singly-polymerized ionic liquids (SPILs) obtained from the same cation and anion, respectively. BDS measurements were carried out as a function of temperature, with measurements made both above and below the glass transition temperatures of the materials. Interestingly, we find not only that the bulk conductivities of the DPIL material are significantly lower than those of the SPILs, as seen in previous work, but their local relaxation timescales are also approximately 4 orders of magnitude slower, as well. As discussed below, the strong ionic interactions between the polymer chains appear to significantly restrict both bulk and local ionic motions, providing exciting new avenues for long-term control of static charge distributions in ion-containing polymers.

Experimental Methods

Materials

All reagents were purchased from standard commercial suppliers (see Supporting Information). Triethylamine was distilled over CaH_2 under inert atmosphere. 3-sulfopropyl methacrylate potassium salt was dried under vacuum for 2 h at 25 °C. AIBN was purified by recrystallization from methanol below 40 °C. All other reagents were used as received.

Synthesis of Singly- and Doubly-Polymerizable Monomers

The polymerized ionic liquid monomers were prepared according to previously reported procedures.[19,41–43]

Briefly, the polymerizable cationic monomer, **SPIL(+)**, was prepared by quaternizing N-methylimidazole with 2-bromoethanol in the absence of solvent in quantitative yield. Subsequent acrylation with methacryloyl chloride at room temperature yielded the polymerizable imidazolium salt. The imidazolium salt was then ion-exchanged with [Li][TFSI] to yield singly-polymerizable ionic liquid **SPIL(+)**.[19,23,41]

The polymerizable anionic monomer, **SPIL(-)**, was prepared by converting potassium 3-(methacryloyloxy)propane-1-sulfonate into its sulfonyl chloride derivative by treatment with thionyl chloride. This product was subsequently converted into a trifluoromethanesulfonamide-based triethylammonium salt. The triethylammonium cation was then ion-exchanged with Li^+ to yield a polymerizable trifluoromethanesulfonamide salt that was finally ion-exchanged with 1-ethyl-3-methylimidazolium bromide to yield the desired singly-polymerizable ionic liquid **SPIL(-)**.[43]

Finally, the doubly polymerizable ionic liquid, **DPIL**, was prepared by ion-exchanging the polymerizable imidazolium salt with the polymerizable trifluoromethanesulfonamide in a salt-metathesis reaction to yield the doubly-polymerizable ionic liquid **DPIL**.[19] Successful synthesis of all products was confirmed by ^{1}H and ^{19}F NMR, as shown in the Supporting Information.

Characterization of the polymerized ionic liquids

Differential Scanning Calorimetry (DSC)

For DSC measurements, the PIL monomers were polymerized directly onto the DSC pan via thermal initiation with azobisisobutyronitrile (AIBN). Briefly, a stock solution of AIBN (6.1 mM) was made in dichloromethane. 10 mg of the PIL monomer was then directly

weighed on the DSC pan. AIBN solution was added to the DSC pans containing the PIL monomers (monomer:initiator = 500:1). The pan was protected from light and dichloromethane was allowed to evaporate. The DSC pan was then carefully placed in a vacuum oven and the samples and were heated at 80 °C overnight. The samples were cooled to room temperature prior to measurement.

The glass transition temperatures (T_g) of the polymerized ionic liquids were then measured with a DSC2500 differential scanning calorimeter (TA Instruments) that was calibrated for temperature and heat flow with indium reference samples provided by the manufacturer. Measurements were performed using heat/cool/heat method under a constant flow rate of nitrogen (50 ml/min). The samples were sealed in a 40 μL hermetic aluminum pan with a Tzero press. An empty pan sealed with a lid was used as the reference. The PILs were first equilibrated for 5 min at -80 °C. They were then heated to 180 °C at a rate of 10 °C/min and held at this temperature for 5 min. The PILs were then cooled to -80 °C at 10 °C/min and held at this temperature for 5 min. The PILs were finally heated again to 180 °C at 10 °C/min. The T_g was determined by the mid-point method on the cooling cycle thermogram.

Broadband Dielectric Spectroscopy

The dielectric response of the polymerized ionic liquids was measured by broadband dielectric spectroscopy. To prepare samples for dielectric measurements, 200 mg of the PIL monomer was weighed in a scintillation vial. A stock solution of AIBN (6.1 mM in dichloromethane) was added to the PIL monomer such that monomer:AIBN = 500:1. The solvent was allowed to evaporate prior to deposition in the BDS sample cell. The cell's brass electrodes were mechanically polished and thoroughly cleaned by sequentially sonicating in methanol followed by acetone prior to the measurements. The prepared sample was then loaded onto the 30 mm diameter bottom electrode with 50 μm silica fiber spacers. The 15 mm diameter top electrode was then placed onto the sample such that the PIL was sandwiched between two

electrodes, forming a parallel plate capacitor. Following deposition, the PIL was polymerized in the sample cell in a vacuum oven at 80 °C overnight. The top electrode was then pressed down by hand to ensure contact with the silica spacers and a consistent thickness of 50 μm, which was verified using calipers. BDS measurements were carried out using a Concept 40 broadband dielectric spectrometer (Novocontrol GmbH). The sample was annealed in the instrument at 130 °C for 1 h under flow of dry nitrogen to ensure complete removal of residual moisture. Frequency sweeps were then carried out at an amplitude of 0.1 V with frequencies ranging from 0.1-10^7 Hz for all experiments. Frequency sweeps were carried out between 130 °C and -150 °C following a cool/heat/cool cycle. For each cycle, the temperature steps were chosen to be 10 °C near the sample's calorimetric T_g and were gradually increased to 30 °C far from T_g.

Results

Monomers and Polymer Synthesis

The chemical structures of the methacrylate-based ionic liquid monomers investigated in this study are shown in Scheme 1. The three polymerizable ionic liquids are (a) a singly-polymerizable imidazolium-based cationic monomer with a mobile Tf_2N^- counterion (referred to as **SPIL(+)**), (b) a singly-polymerizable trifluoromethylsulfonimide-based anionic monomer with a mobile $EMIM^+$ counterion (referred to as **SPIL(-)**), and (c) a doubly-polymerizable ionic liquid containing both the polymerizable cation and the polymerizable anion without any mobile counterions (referred to as **DPIL**). The synthesis of these SPIL and DPIL monomers has been described previously.[19,23,41,43] The PIL monomers were all viscous liquids at room temperature. Following polymerization, the SPIL samples yielded very soft solids, while the DPIL yielded a hard, rigid material that was insoluble in both polar and nonpolar solvents.

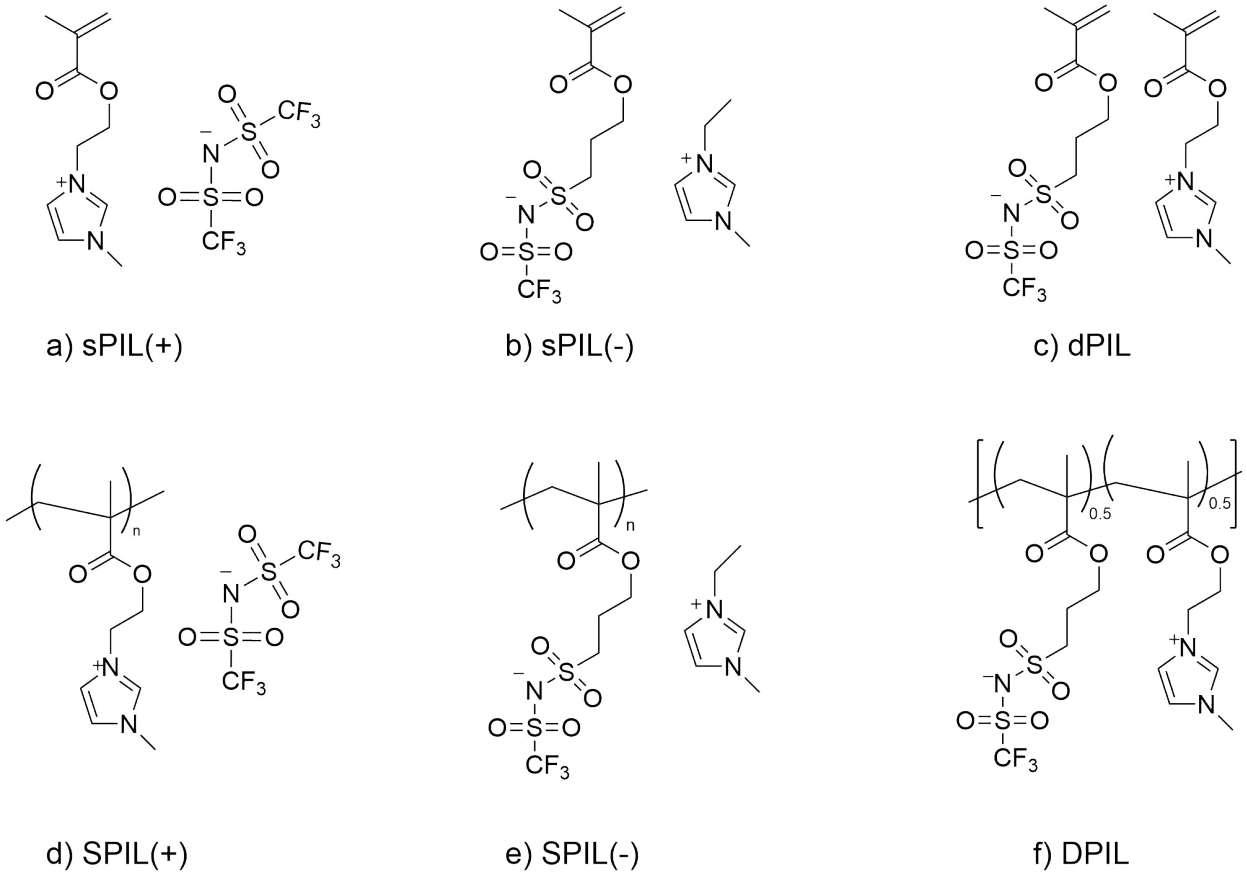

Scheme 1: Chemical structures of polymerizable ionic liquid monomers (a-c) and their corresponding polymers (d-f) investigated in the present work.

Thermal Characterization

The glass transition temperatures (T_g's) of the polymerized ionic liquids were measured using differential scanning calorimetry (DSC). DSC profiles of the polymerized SPILs and DPIL are shown in Figure 1. All of the polymer samples displayed broad glass transition temperatures within the scan range, as indicated by the arrows and summarized in Table 1. As seen in this data, the T_g of SPIL(+), at 13 °C (286 K), was approximately 50 °C higher than that of SPIL(-), while that of the DPIL was even higher, at 75 °C (348 K).

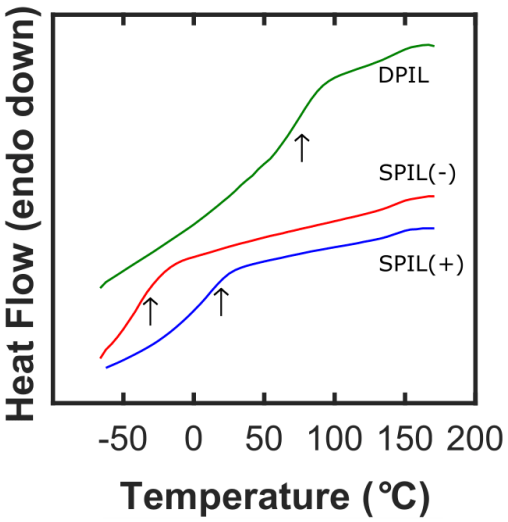

Figure 1: DSC thermograms of PILs obtained during the cooling cycle of the DSC run. Arrows indicate the glass transition temperatures of each material. Complete DSC profiles including both the heating and cooling cycles are included in the Supporting Information.

Table 1: Glass Transition Temperatures of Polymerized Ionic Liquids from DSC and BDS Measurements

Sample	**DSC T_g (K)**	**BDS T_g (K)**[a]
SPIL(+)	286	260
SPIL(−)	236	236
DPIL	348	331

[a]Reported as the temperature at which the frequency of of ion pair relaxations reaches 0.01 rad/s - see section on Dielectric Relaxations for details

While the insolubility of the DPIL in standard NMR solvents prevented direct assessment

of the monomer conversion, the absence of a polymerization exotherm in the DSC trace suggested the successful polymerization of the majority of the PIL monomers. The DSC thermograms of the polymers also did not show any signatures of crystallization or melting during the thermal cycle. Finally, all of the polymerized ionic liquids were found to be thermally stable up to at least 180 °C, with no signs of thermal decomposition observed in the DSC profile.

Ionic Conductivity

Changes to the bulk ion transport properties of the samples upon polymerisation of one or both ionic species were quantified via the measured conductivities of the samples. The frequency dependence of the real part of the conductivity, σ', is shown as a function of temperature in Figure 2 for all three PIL materials. As shown in this figure, σ' generally increases with increasing frequency. At high temperatures, each trace exhibits a distinct plateau corresponding to DC conductivity, as discussed in more detail, below. At frequencies below this plateau, a decrease in σ' is observed. In the SPIL samples, this response is attributed primarily to electrode polarization, which reflects a build-up of mobile ions at the electrodes that in turn decreases the field felt by ions in the bulk of the material and consequently decreases its apparent conductivity.[32,44,45] This signature is prominent in the SPILs (Fig. 2a,b), but is not seen in the DPILs even at the lowest frequencies measured (Fig. 2c), qualitatively indicating a significant decrease in the ability of ions to move toward the electrode interfaces. Although the DPIL materials should still exhibit a small capacitative response at low frequencies even in the absence of mobile ions, this response was not observed within the experimental frequency window.

The characteristic DC conductivity, σ_{DC}, of the sample at each temperature can be obtained from the value of σ' across the plateau at intermediate frequencies.[33,46] The extracted DC conductivity of each sample across the entire temperature range in this work is shown in Figure 3. As seen in this figure, the ionic conductivity increases with increasing temperature.

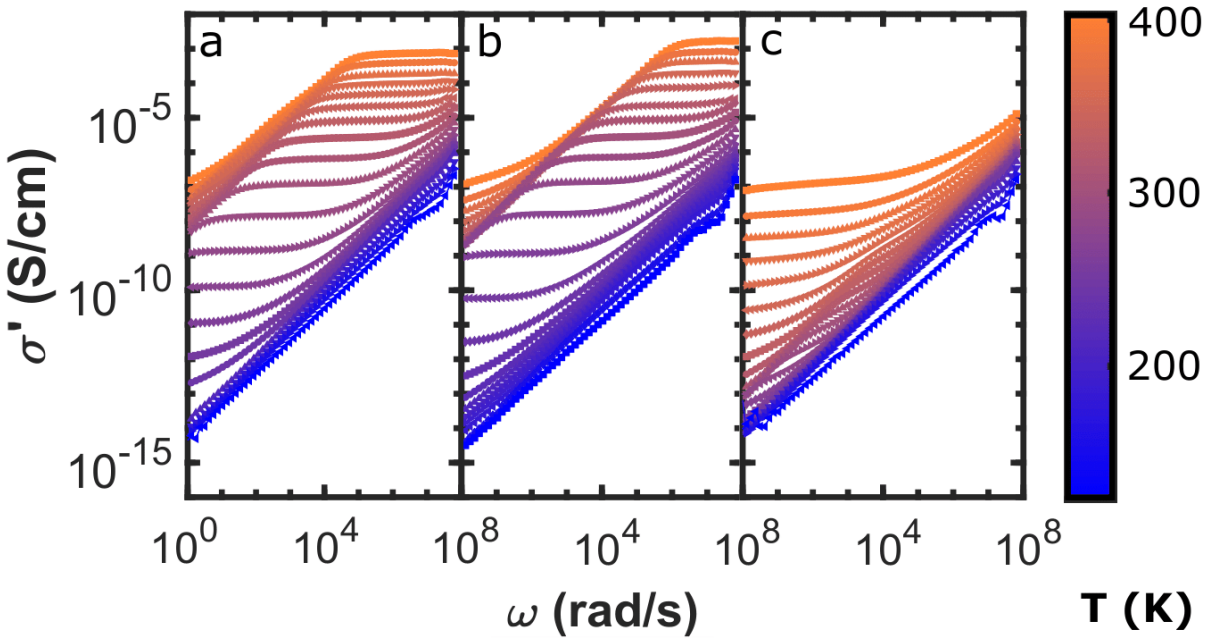

Figure 2: Plot of the real part of the conductivity (σ') of (a) SPIL(+), (b) SPIL(-), and (c) DPIL as a function of angular frequency across the range of temperatures investigated in this work.

SPIL(-) has a slightly higher conductivity than SPIL(+) across the temperature range, while the DC conductivity of the DPIL was more than 4 orders of magnitude lower, as discussed in more detail, below. For the SPILs, the temperature-dependent DC conductivities were fit to the Vogel-Fulcher-Tammann (VFT) equation above the T_g of the materials.[47] The VFT fits had the form

$$\sigma_{DC} = \sigma_\infty \exp\left(\frac{-DT_0}{T - T_0}\right) \tag{1}$$

where T_0 is the Vogel temperature, σ_∞ is the ionic conductivity at infinite temperature, and D is the strength index describing the strength of temperature dependence of relaxation time.[48,49] The fitted values of these parameters are summarized in Table 2. As seen in Figure 3, the conductivity of both SPILs was well-described by VFT dynamics above their glass transition temperatures, with T_0 values approximately 45-70 K below the DSC glass transition temperature,[50] in reasonable agreement with previously published work on

imidazolium-based methacrylate polymers with BF_4^- and TFSI counterions.[38] The conductivity of SPIL(-) correlates well with SPIL(+), indicating that these materials have similar ion transport mechanisms, as expected for polymerized ionic liquids with similar chemistries.

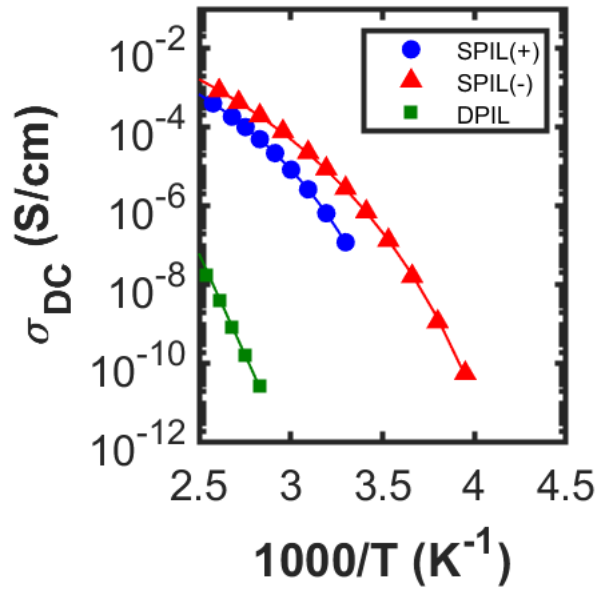

Figure 3: Temperature dependence of DC conductivity of PILs with Arrhenius fit for DPIL as solid line and VFT fits for SPILs as solid curves above T_g.

Table 2: Fit Parameters for the DC conductivity of polymerized ionic liquids above their glass transition temperatures

PILs	σ_∞ (S/cm)	**D**	$\mathbf{T}_0$ (K)	$\mathbf{E}_a$ (kJ/mol)
SPIL(+)[a]	1.29	6.26	219	-
SPIL(−)[a]	3.16	8.44	189	-
DPIL [b]	2.5×10^{18}	-	-	196

[a] VFT fit, [b] Arrhenius fit

In contrast to both SPIL systems, the DC conductivity of the DPIL was not well-described by VFT dynamics. The DC conductivity of the DPILs was instead fit to an Arrhenius form

$$\sigma_{DC} = \sigma_\infty \exp\left(-\frac{E_a}{RT}\right) \tag{2}$$

where E_a is the activation energy for ion conduction and σ_∞ is the predicted high-temperature

limit of the conductivity. The resulting fit parameters are summarized in Table 2. Interestingly, the fitted value of the prefactor σ_∞ is unphysically large, suggesting that the Arrhenius behavior may break down at higher temperatures than investigated here.

Dielectric Permittivity

Following characterization of the bulk ion transport, local relaxations were investigated using the dielectric permittivity, ϵ. The real parts of the dielectric permittivities of each sample, ϵ', and their derivative spectra at different temperatures, are shown as a function of frequency in Figure 4. As seen in panels (a), (b), and (c), ϵ' decreases with increasing frequency. The electrode polarization appears as a strongly negative-sloped region at low frequencies, and dominates the dielectric spectra of the SPILs in the low-frequency portion of the spectrum. As observed in the conductivity, the DPIL has a much weaker contribution from electrode polarization, with the spectrum only exhibiting signatures of this response above the material's T_g. The dielectric spectra of all three PILs show distinct signatures of relaxational processes in the measured frequency range, which appear as steps in the real part of the dielectric response that shift toward higher frequencies with increasing temperatures as the relaxations speed up. Consistent with previous work on similar polymerized ionic liquid systems, this relaxation process was attributed to reorientation of ion pairs within the material.[33,51–53]

Dielectric Relaxations

The derivative formalism was applied to remove contributions from ionic conductivity and allow the relaxations to be resolved, as has been reported previously.[26,50,54] The derivative of the real part of the permittivity with respect to frequency was calculated using[55,56]

$$\epsilon_{der} = -\frac{\pi}{2}\frac{\partial \epsilon'(\omega)}{\partial \ln \omega} \tag{3}$$

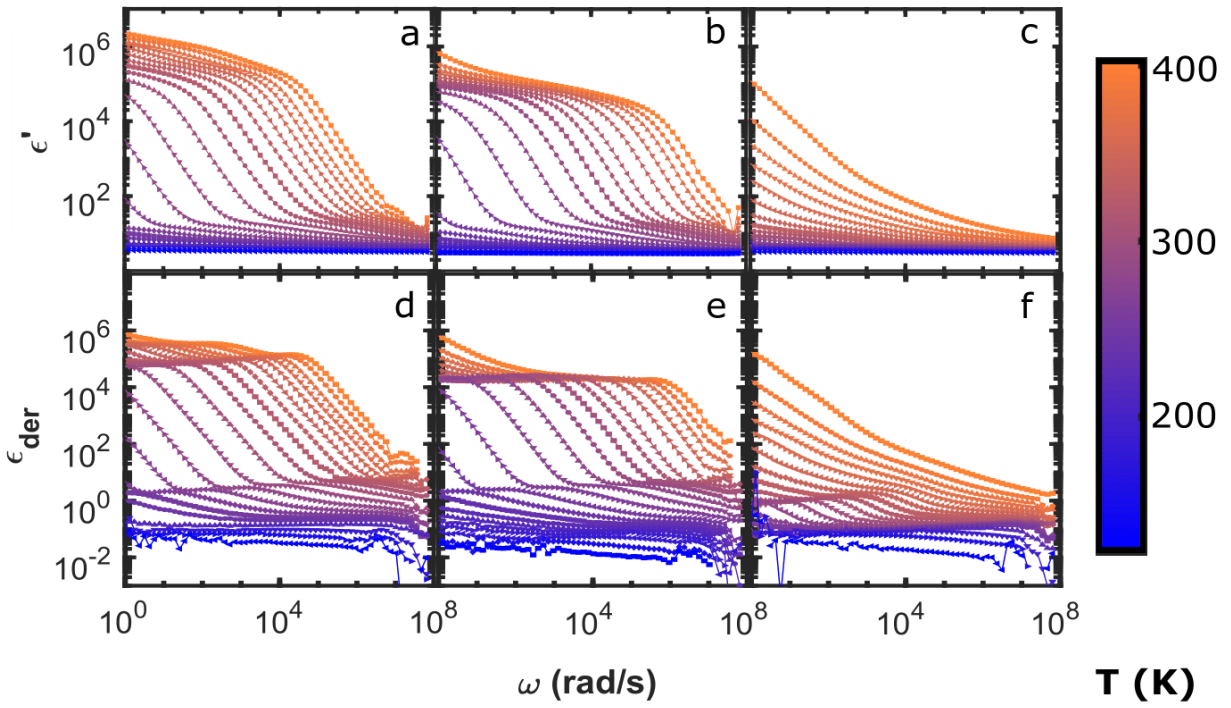

Figure 4: Frequency dependence of (a-c) the dielectric permittivity and (d-f) the dielectric loss derivative function ϵ_{der} for (a, d) SPIL(+), (b, e) SPIL(-), and (c, f) DPIL across the range of temperatures investigated in this work.

As shown in Figure 4(d-f), in the derivative spectra, the broad steps in ϵ' are transformed into distinct peaks that broaden and shift to higher frequencies with increasing temperature. Quantitative information about the timescales of the dipolar relaxations was then obtained by fitting the derivative spectra with a combination of a power-law electrode polarization response and Havriliak-Negami (HN) functions representing dielectric relaxations.[26] In previous work on similar SPIL systems, two HN functions have been required to fully represent the dielectric response, including one (α_2) at lower frequency that is typically attributed to ion pair rearrangement, and a second (α) at higher frequency that is attributed to segmental motion of the polymer chains.[29,37,38] In the present data, however, we found that the higher frequency α mode was too broad to be accurately fit, and the response was instead analyzed using a single HN function with a constant offset to account for broad, low-amplitude relaxations remaining at high frequency. Thus, the function used to fit the derivative spectra

was

$$\epsilon_{der} = A\omega^{-s} - \frac{\pi}{2}\left[\frac{\partial \epsilon'_{HN}(\omega)}{\partial\, ln\, \omega}\right] + C \tag{4}$$

where A and s are the constants representing the amplitude and power-law dependence of the contribution to ϵ_{der} from the electrode polarization, C is a small constant offset, and $\epsilon'_{HN}(\omega)$ is a Havriliak-Negami function of the form

$$\epsilon'_{HN}(\omega) = \mathrm{Re}\left\{\frac{\Delta\epsilon}{[1 + (\frac{i\omega}{\omega_{HN}})^a]^b}\right\} \tag{5}$$

where $\Delta\epsilon$ is the relaxation strength of the corresponding relaxation mode, a and b are the shape parameters, and ω_{HN} is the angular frequency. For the HN relaxation mode, the parameters a, b, and ω_{HN} can also be used to calculate the frequency of maximal loss ω_{max}, given by[26]

$$\omega_{max} = \omega_{HN}\left(\sin\frac{a\pi}{2+2b}\right)^{\frac{1}{a}}\left(\sin\frac{ab\pi}{2+2b}\right)^{-\frac{1}{a}} \tag{6}$$

The frequency of maximal loss is used instead of ω_{HN} to analyze the temperature dependence of the relaxation timescale to account for asymmetries in the relaxation spectrum.[57,58] Representative fits of derivative spectra of each sample to the functional form given in Equation 4 are shown in Figure 5.

To minimize the number of fitting parameters and improve the reproducibility of the fits, the values of s, a, and b were fixed to the values given in the caption of Figure 5. The shape parameters in the HN function, a and b, were fixed to the values obtained from fitting the response at the temperature at which the HN relaxation was most pronounced; because the α_2 relaxation is expected to have the same peak shape at different temperatures, the same a and b values were used over the entire temperature range.[59] For the SPILs, the power law exponent, s, representing the contribution from electrode polarization was fixed to a value chosen by taking the average of all the s values over the entire temperature range, as reported for similar ionomer systems.[29,37,38] For the DPIL, the electrode polarization was not well-described with a fixed value of this parameter, and s was allowed to vary. Interestingly, the

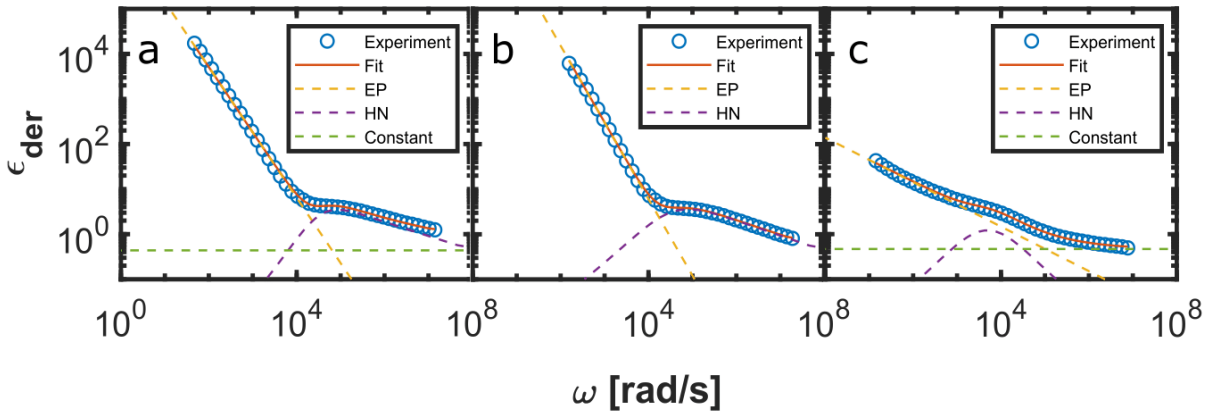

Figure 5: Dielectric loss derivative spectra at T_g fit to the sum of a power law for EP and derivative form of HN function for ion rearrangement of (a) SPIL(+), (b) SPIL(-), and (c) DPIL. The solid curves are three-parameter fits to Eqn. 4 with following values of s, a, and b for (a) SPIL (+): $s = 1.45$, $a = 0.9$, $b = 0.34$ (b) SPIL (-): $s = 1.7$, $a = 0.74$, $b = 0.45$ (c) DPIL: s=Varied, $a = 0.76$, $b = 1.0$.

resulting values, which fell between 0.2 and 0.5, are significantly lower than those obtained for either SPIL system, again reinforcing the idea that the low-frequency behavior in the DPIL system is not well-described by electrode polarization models developed for materials containing mobile ions of one charge.

The fitted values of the relaxation peak frequency, ω_{max}, and the relaxation strength, $\Delta\epsilon$, are shown in Figures 6 and 7. The dynamics of SPIL(-) were too slow below T_g to be captured in the frequency range studied. For the DPIL, the relaxations became too broad at higher temperatures to be accurately fit independent of the electrode polarization background. For all datasets for which ω_{max} could be reliably extracted, the temperature dependences of were fit to VFT ($T > T_g$) and Arrhenius ($T < T_g$) dynamics above and below the measured glass transition temperatures, respectively:[37]

$$\omega_{max} = \omega_\infty \exp\left(-\frac{DT_0}{T - T_0}\right) \text{ for } T > T_g \tag{7}$$

$$\omega_{max} = \omega_\infty \exp\left(-\frac{E_a}{RT}\right) \text{ for } T < T_g \tag{8}$$

Here, ω_∞ is the high-temperature limiting frequency, D is the strength parameter for the relaxation, T_0 is the Vogel temperature, E_a is the activation energy for ion pair rearrangement, and R is the universal gas constant. The resulting fits are shown in Figure 6, and the fit parameters are summarized in Table 3.

Table 3: Fitting Parameters for the Arrhenius (T<T_g) and VFT (T>T_g) temperature dependence of the ion rearrangement frequencies obtained from fits to ϵ_{der}

PILs	**T > T_g**			**T < T_g**	
	ω_∞ (rad/s)	**D**	T_0 (K)	E_a (kJ/mol)	ω_∞ (rad/s)
SPIL(+)	3.93×10^{11}	5.89	219[a]	146.3	1.74×10^{30}
SPIL(−)	1.11×10^{12}	8.07	189[a]	-	-
DPIL	1.49×10^{4}	0.12	328	94.4	3.89×10^{17}

[a] T_0 values for SPIL(+) and SPIL(-) were fixed to the values obtained from fits to σ_{DC}

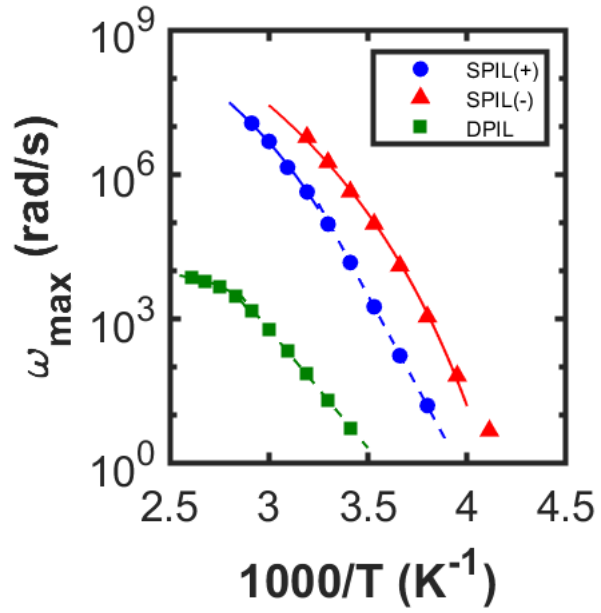

Figure 6: Temperature dependence of relaxation frequency maxima, ω_{max}, obtained from fits to ϵ_{der}. Overlaid curves indicate fits to an Arrhenius model (dashed lines) below T_g and a VFT model (solid curves) above T_g.

For the SPIL samples, the value of T_0 was fixed to the same value obtained from the fits to σ_{DC} (Table 2), while for the DPIL sample, for which the σ_{DC} data did not follow

VFT dependence above T_g, the value of T_0 was allowed to vary. The obtained value of T_0 for the DPIL was somewhat closer to the materials' calorimetric T_g than observed in the SPILs, with $T_g - T_0 \approx 20$ K. In the DPIL, in which both ionic species were immobilized, the relaxation process was also up to 4 orders of magnitude slower than in the SPILs. Interestingly, the activation energy obtained for the DPIL was approximately 35% lower than that for SPIL(+), suggesting that the individual ion pairs may be more weakly bound in the DPIL, even if the overall relaxation rate is slower. The dynamic T_g's listed in Table 1 were found by extrapolation of the VFT fits of the relaxation process to 0.01 rad/s.[60] There is a reasonable agreement between the BDS T_g and DSC T_g for all three materials. The T_g of SPIL(+) extracted from BDS is approximately 26 K lower than that obtained via DSC, while for SPIL(-), there was no measurable difference. The mismatch is similar for the DPIL, at 17 K, placing the values for all three systems well within the range observed in other polymerized ionic liquid materials.[37,59] We note that this difference likely arises because the glass transition is a kinetic phenomenon, and as such, depends on the cooling rate at which the experiment is conducted.[61] Because the cooling rate was faster in the DSC thermal analysis (10 K/min) than in the BDS experiments (averaging 0.1 K/min), it is expected that DSC should yield a higher T_g, as observed here.

The temperature dependence of the relaxation strengths for each PIL is shown in Figure 7. For the SPILs, the relaxation strengths increase with increasing temperature. This trend is consistent with similar previously-reported imidazolium-based ionomers.[29,37,38] Interestingly, SPIL(-) had a larger $\Delta\epsilon_{\alpha 2}$ than SPIL(+), likely reflecting greater flexibility in the longer sidechain. The magnitude of the relaxation strength (8-23) in the SPILs is on the lower end of the range of relaxation strengths observed in other polymerized systems (20-120).[27,50,54] On the other hand, for the DPIL, $\Delta\epsilon_{\alpha 2}$ is much smaller than in the SPILs, with a value of only 2-3, and has a much weaker temperature dependence.

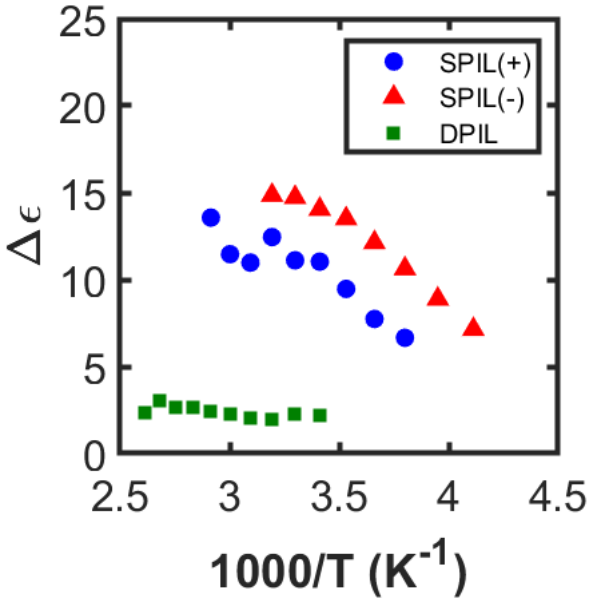

Figure 7: Temperature dependence of relaxation strengths $\Delta\epsilon$ corresponding to ion-rearrangements process for all investigated PILs.

Static Dielectric Constant

The final important characteristic of the PILs investigated in this work is the static dielectric constant, ϵ_s. The static dielectric constant reflects the polarity of the molecule and, in the absence of electrode polarization, should appear as a plateau in the dielectric response at low frequency.[62,63] In the presence of mobile ions, however, electrode polarization overwhelms the static response at low frequencies. To address this problem, ϵ_s for all three types of polymerizable ionic liquids was estimated from the sum of the relaxation strengths of any molecular relaxations and the high frequency dielectric permittivity values.[29,62] For comparison with work on other polymerized ionic liquid systems, ϵ_s for both SPIL samples was also estimated using

$$\epsilon_s = \frac{\tau_\sigma \sigma_{DC}}{\epsilon_0} \tag{9}$$

where τ_σ is the conduction timescale extracted from electrode polarization analysis (see Supporting Information) and σ_{DC} is the DC conductivity obtained from the plateau in σ', as discussed above.[44,64,65]

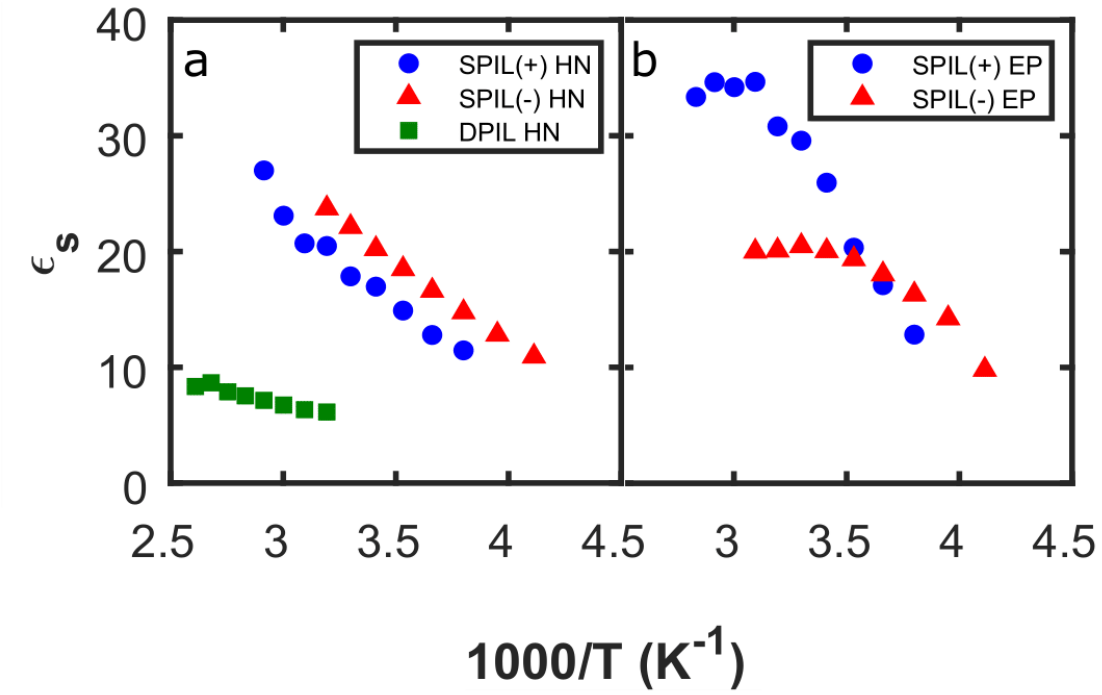

Figure 8: Temperature dependence of static dielectric constant for all PILs in the current study calculated by (a) HN fitting of dielectric loss derivative spectra, and (b) electrode polarization analysis.

The resulting temperature dependence of ϵ_s obtained from both methods is shown in Figure 8. For SPILs, unexpectedly, the temperature dependence of ϵ_s calculated using the two different approaches was markedly different. The values of ϵ_s calculated using the electrode polarization timescales and conductivities (Fig. 8(b)) appeared to pass through a maximum at intermediate temperatures, and SPIL(+) had a higher value of ϵ_s than SPIL(-) across most of the temperature range. On the other hand, the values of ϵ_s calculated by the summation of HN relaxation strength and high frequency value of ϵ' (Fig. 8(a)) increase monotonically with increasing temperature. Additionally, SPIL(-) has a higher ϵ_s than SPIL(+) across the entire temperature range, in contrast to the result obtained from the electrode polarization analysis. This discrepancy highlights limitations in the electrode polarization approach to obtaining ϵ_s, as discussed below.

Discussion

The small number of previous reports on doubly-polymerized ionic liquid and ionic liquid copolyampholytes have noted a significant decrease in conductivity relative to conventional polymerized ionic liquids, consistent with the results presented here. The room-temperature DC conductivity of the DPIL investigated in this work was below 10^{-13} S/cm, comparable to values obtained by Yoshizawa et al. (10^{-9} S/cm for a vinyl-type DPIL[22]) and Shaplov et al. (10^{-12}-10^{-10} S/cm for a methacrylate copolyampholyte after removal of free counterions[23]). However, in this previous work, the molecular-scale origin of the observed decrease in bulk ion transport was not clear: is it due simply to the conversion of small, mobile molecular ions to large, immobile polymeric chains? Or do strong ionic interactions between the chains play an important role, as seen in polyampholyte gels[66]?

Here, thorough calorimetric and impedance spectroscopy characterization of a family of SPILs and their chemically-related DPIL help shed light on this question, as well as bring insight into the more local motions that are not resolved in bulk conductivity measurements.

As discussed below, the data presented here is most consistent with a picture in which the copolymerization of the two ionic species leads to ionic interactions between the chains that serve as ionic crosslinks analogous to those seen in polyampholyte gels,[66] and significantly hinder ion transport in the material.

The glass transition temperatures and physical characteristics of the polymerized DPIL provide the first piece of evidence supporting this picture. The DPIL material had a higher T_g than either SPIL, and was a brittle solid that was insoluble in all common laboratory solvents and could not successfully be hot-pressed even 105 K above its glass transition temperature. The insolubility of the material, and its lack of thermoplasticity, are more consistent with the behavior expected for crosslinked solids than non-interacting polymer chains. Comparison of the T_g value measured for the DPIL to those measured for the SPILs is also informative. At first glance, the DPIL appears to be a statistical copolymer of SPIL(+) and SPIL(-). In this case, the T_g of the material should be well-predicted by the Fox equation,[67]

$$\frac{1}{T_g} = \frac{w_1}{T_{g1}} + \frac{w_2}{T_{g2}} \tag{10}$$

where T_g is the predicted glass transition temperature of the copolymer, w_1 and w_2 are the weight fraction of monomer 1 and 2 in the copolymer, and T_{g1} and T_{g2} are the glass transition temperatures of homopolymers 1 and 2. If applied to the present system, this approach predicts that DPIL's T_g should be approximately 260 K. The observed T_g of the DPIL, however, is 386 K, roughly 120 K higher than the predicted value. On closer inspection, however, this disagreement is not surprising because the DPIL is not actually a copolymer of the two SPILs, as it lacks their mobile counterions. In their absence, the strong interactions between the two charged monomers effectively serve as crosslinks, making the structure more rigid and increasing the T_g. In this context, including a stoichiometric amount of non-polymerizable [EMIM][TFSI] would be expected to reduce the T_g of the DPIL to a value consistent with the Fox equation and significantly soften the material, which will

be investigated in future work. Finally, we note that although only the cooling cycle of the DSC run is shown in Figure 1 for consistency with the BDS data, the DSC profile of DPIL revealed that the T_g of this material shifted approximately 9 K after being cycled to high temperature (see Supporting Information); this shift was observed only in the DPIL system, and was not seen for either of the SPILs. This observation suggests that thermal polymerization of the DPIL at 353 K may effectively generate a supercooled, crosslinked glass with a different molecular organization than produced by annealing pre-formed ionic liquid copolyampholyte materials cooled from a higher temperature.

Results from the BDS experiments reinforce the idea that the properties of the DPIL materials are dominated by the ionic interactions between the chains. While the DC conductivities of both SPIL samples are comparable to those measured in other polymerized ionic liquid systems, the conductivity of the DPIL was 4-5 orders of magnitude lower, reflecting significantly hindered ion transport. Although we cannot definitively determine the origin of the small residual conductivity, we suspect that it arises from long-range motion of a small number of residual unreacted monomers. Interestingly, the temperature dependence of the DC conductivity was best described using an Arrhenius model rather than VFT dynamics, even above the material's T_g. This result suggests that the ion transport process in the DPIL is some form of activated hopping mechanism, rather than dependent solely on the amount of free volume available at each temperature. Additionally, the activation energy obtained from the fit is approximately twice that obtained for ion pair relaxation of the same material below T_g. Both of these pieces of data suggest that the ion transport mechanism relies on simultaneous relaxation of multiple ion pairs, consistent with the picture of the DPIL as an extensively ionically-crosslinked material even above its T_g. We do note that the Arrhenius model yielded an unphysically high value of σ_∞, suggesting that this model may break down above the temperature range accessed here; however, even if the conductivity transitions to VFT-like behavior at higher temperatures, the T_0 value would necessarily be much higher than seen in the analysis of the individual local relaxations, indicating that ion

transport is decoupled from the local relaxations in the DPIL material.

The relaxation frequencies and relaxation strengths extracted from the dielectric relaxation analysis provide further insight into the extent to which local ionic motions are restricted in the DPIL materials. The ion pair relaxation rate in the DPIL was significantly slower than in the SPIL, and the relaxation strength significantly smaller. The relaxation strength is particularly informative, as it reflects the ion pairs' ability to reorient in response to an applied field. Here, the low relaxation strength observed in the DPIL indicates that the ion pairs physically cannot reorient to the extent that ion pairs in the SPILs can. While ion pair relaxation in the SPILs may proceed via hopping of the mobile counterions independent of other ion pairs,[31,68] in the DPILs, the chain connectivity means that relaxation of any individual ion pair also requires rearrangement of other nearby ion pairs. The ions in each ion pair in the DPIL effectively have very few degrees of freedom for independent motion, hindering their response to the applied field and reducing the relaxation strength.

Finally, we note that the lower static dielectric constant observed in the DPILs relative to the SPILs is largely a result of their reduced local relaxation strength. Interestingly, we observe that the values of ϵ_s calculated from the fits to ω_{max} increase with increasing temperature. However, for the SPILs, values of ϵ_s calculated independently from analysis of the electrode polarizations (see Supporting Information) increase and then drop off again with increasing temperature, as expected as the increase in available thermal energy and free volume first makes it easier for the dipoles to reorient, before thermal randomization of the dipoles begins to dominate the response.[69–71] Although we cannot positively identify the source of this discrepancy from the present data, we suspect that the mismatch arises from the fact that the MacDonald model used in the electrode polarization analysis ignores the interactions between ions.[50,72] In polymerized ionic liquids, however, the ion density is high, and it may not be appropriate to ignore these interactions. While we expect a similar effect would be observed in the DPIL, analogous analysis could not be carried out for the DPILs because the width of the $\tan\delta$ peaks prevented robust fitting of the DPIL

data to the MacDonald-Coelho model (see Supporting Information). However, application of the MacDonald-Coelho model to this system is likely inappropriate in any case. One of the inherent assumptions of MacDonald-Coelho model is that the system contains a mobile counterion,[54,64,73,74] but this assumption fails in the DPIL, in which both ions are immobilized due to their attachment to the polymer chain. Complete analysis of the electrode polarization process in the DPIL would require development of a model that is more suitable for these systems.

Our results thus paint a picture of the DPILs as materials in which extensive ionic interactions between chains significantly hinder both bulk and local ionic motions. The material is effectively physically crosslinked, and ion motion requires cooperative rearrangement of multiple ionic crosslinks at the same time. We expect that a similar molecular-scale description will apply to other DPIL or ionic liquid copolyampholyte materials; however, a significant number of molecular factors, including the presence of free or unpolymerized ions, different ion chemistries and linker flexibilities, and incorporation of non-ionic monomers may mediate the ion transport and local relaxations in these systems. Exploring these factors thus offers a number of exciting directions for future work that will significantly enhance both our physical understanding of these materials and their potential device applications.

Conclusion

We have demonstrated that tethering both of the ionic species in a polymerizable ionic liquid to the polymer backbone generates a significantly different dielectric response than in conventional singly-polymerized ionic liquids. The effect of polymerizing both of the ionic species in the DPIL is clearly observed in both the glass transition temperature and conductivity; the DPIL has higher T_g and significantly lower ionic conductivity than its SPIL counterparts. Additionally, the relaxation spectra of SPILs exhibit characteristic signatures of ion conduction and electrode polarization that are missing in the DPIL sample. Looking

beyond the ionic conductivity, the molecular-scale relaxations of the DPIL were also much slower and had lower relaxation strengths for ion-pair rearrangements than observed in either of the SPILs. The weak relaxation strengths of the DPIL resulted in a lower value of the static dielectric constant, and further strengthen our conclusion that polymerization of both ionic species hinders the dipoles from responding to the applied field, even when both are attached to the polymer backbones via relatively flexible linkers. Taken together, our results indicate that ionic crosslinking is responsible for the "ion-locking" phenomenon in DPILs. Further exploration of the chemical and physical factors controlling this phenomenon should help guide design of DPIL materials for applications requiring significant restriction of ion transport in ion-containing polymers, and provide further detailed insights into the molecular-scale mechanisms of this behavior.

Acknowledgement

The authors thank Robert Hickey and Wenwen Mei for assistance with collection of the BDS data, and Susan Fullerton-Shirey and Jerry Liang for helpful discussion. This material is based on work supported by the Air Force Office of Scientific Research under AFOSR award number FA9550-19-1-0196. This work was performed, in part, at the Nanoscale Fabrication and Characterization Facility, a laboratory of the Gertrude E. and John M. Petersen Institute of NanoScience and Engineering, housed at the University of Pittsburgh.

Supporting Information Available

Materials; full DSC traces for all samples; electrode polarization analysis of SPILs.

References

(1) Mecerreyes, D. Polymeric ionic liquids: Broadening the properties and applications of polyelectrolytes. *Progress in Polymer Science* **2011**, *36*, 1629–1648.

(2) Green, M. D.; Long, T. E. Designing Imidazole-Based Ionic Liquids and Ionic Liquid Monomers for Emerging Technologies. *Polymer Reviews* **2009**, *49*, 291–314.

(3) Snedden, P.; Cooper, A. I.; Scott, K.; Winterton, N. Cross-Linked Polymer-Ionic Liquid Composite Materials. *Macromolecules* **2003**, *36*, 4549–4556.

(4) Yuan, J.; Mecerreyes, D.; Antonietti, M. Poly(ionic liquid)s: An update. *Progress in Polymer Science* **2013**, *38*, 1009–1036.

(5) Shaplov, A. S.; Ponkratov, D. O.; Vygodskii, Y. S. Poly(ionic liquid)s: Synthesis, properties, and application. *Polymer Science Series B* **2016**, *58*, 73–142.

(6) Qian, W.; Texter, J.; Yan, F. Frontiers in poly(ionic liquid)s: syntheses and applications. *Chemical Society Reviews* **2017**, *46*, 1124–1159.

(7) Hwang, H. J.; Chi, W. S.; Kwon, O.; Lee, J. G.; Kim, J. H.; Shul, Y.-G. Selective Ion Transporting Polymerized Ionic Liquid Membrane Separator for Enhancing Cycle Stability and Durability in Secondary Zinc–Air Battery Systems. *ACS Applied Materials & Interfaces* **2016**, *8*, 26298–26308.

(8) Nykaza, J. R.; Savage, A. M.; Pan, Q.; Wang, S.; Beyer, F. L.; Tang, M. H.; Li, C. Y.; Elabd, Y. A. Polymerized ionic liquid diblock copolymer as solid-state electrolyte and separator in lithium-ion battery. *Polymer* **2016**, *101*, 311–318.

(9) Moon, H. C.; Kim, C.-H.; Lodge, T. P.; Frisbie, C. D. Multicolored, Low-Power, Flexible Electrochromic Devices Based on Ion Gels. *ACS Applied Materials & Interfaces* **2016**, *8*, 6252–6260.

(10) Watanabe, M.; Thomas, M. L.; Zhang, S.; Ueno, K.; Yasuda, T.; Dokko, K. Application of Ionic Liquids to Energy Storage and Conversion Materials and Devices. *Chemical Reviews* **2017**, *117*, 7190–7239.

(11) Seo, D. G.; Moon, H. C. Mechanically Robust, Highly Ionic Conductive Gels Based on Random Copolymers for Bending Durable Electrochemical Devices. *Advanced Functional Materials* **2018**, *28*, 1706948.

(12) Misra, R.; McCarthy, M.; Hebard, A. F. Electric field gating with ionic liquids. *Applied Physics Letters* **2007**, *90*, 052905.

(13) Fujimoto, T.; Awaga, K. Electric-double-layer field-effect transistors with ionic liquids. *Physical Chemistry Chemical Physics* **2013**, *15*, 8983.

(14) Ohno, H.; Ito, K. Room-Temperature Molten Salt Polymers as a Matrix for Fast Ion Conduction. *Chemistry Letters* **1998**, *27*, 751–752.

(15) Washiro, S.; Yoshizawa, M.; Nakajima, H.; Ohno, H. Highly ion conductive flexible films composed of network polymers based on polymerizable ionic liquids. *Polymer* **2004**, *45*, 1577–1582.

(16) Xue, Z.; Qin, L.; Jiang, J.; Mu, T.; Gao, G. Thermal, electrochemical and radiolytic stabilities of ionic liquids. *Physical Chemistry Chemical Physics* **2018**, *20*, 8382–8402.

(17) Ohno, H.; Yoshizawa, M.; Ogihara, W. Development of new class of ion conductive polymers based on ionic liquids. *Electrochimica Acta* **2004**, *50*, 255–261.

(18) Yoshizawa, M.; Ohno, H. Synthesis of molten salt-type polymer brush and effect of brush structure on the ionic conductivity. *Electrochimica Acta* **2001**, *46*, 1723–1728.

(19) Arora, S.; Liang, J.; Fullerton-Shirey, S. K.; Laaser, J. E. Triggerable Ion Release in Polymerized Ionic Liquids Containing Thermally Labile Diels–Alder Linkages. *ACS Materials Letters* **2020**, *2*, 331–335.

(20) Liang, J.; Xu, K.; Arora, S.; Laaser, J. E.; Fullerton-Shirey, S. K. Ion-Locking in Solid Polymer Electrolytes for Reconfigurable Gateless Lateral Graphene p-n Junctions. *Materials* **2020**, *13*, 1089.

(21) Peters, E. C.; Lee, E. J. H.; Burghard, M.; Kern, K. Gate dependent photocurrents at a graphene p-n junction. *Applied Physics Letters* **2010**, *97*, 193102.

(22) Yoshizawa, M.; Ogihara, W.; Ohno, H. Novel polymer electrolytes prepared by copolymerization of ionic liquid monomers. *Polymers for Advanced Technologies* **2002**, *13*, 589–594.

(23) Shaplov, A. S.; Vlasov, P. S.; Lozinskaya, E. I.; Ponkratov, D. O.; Malyshkina, I. A.; Vidal, F.; Okatova, O. V.; Pavlov, G. M.; Wandrey, C.; Bhide, A.; Schönhoff, M.; Vygodskii, Y. S. Polymeric Ionic Liquids: Comparison of Polycations and Polyanions. *Macromolecules* **2011**, *44*, 9792–9803.

(24) Gu, H.; Yan, F.; Texter, J. Polymerized Paired Ions as Polymeric Ionic Liquid-Proton Conductivity. *Macromolecular Rapid Communications* **2016**, *37*, 1218–1225.

(25) Fouillet, C. C. J.; Greaves, T. L.; Quinn, J. F.; Davis, T. P.; Adamcik, J.; Sani, M.-A.; Separovic, F.; Drummond, C. J.; Mezzenga, R. Copolyampholytes Produced from RAFT Polymerization of Protic Ionic Liquids. *Macromolecules* **2017**, *50*, 8965–8978.

(26) Kremer, F., Schönhals, A., Eds. *Broadband Dielectric Spectroscopy*; Springer Berlin Heidelberg, 2003.

(27) Nakamura, K.; Saiwaki, T.; Fukao, K. Dielectric Relaxation Behavior of Polymerized Ionic Liquid. *Macromolecules* **2010**, *43*, 6092–6098.

(28) Iacob, C.; Matsumoto, A.; Brennan, M.; Liu, H.; Paddison, S. J.; Urakawa, O.; Inoue, T.; Sangoro, J.; Runt, J. Polymerized Ionic Liquids: Correlation of Ionic Conduc-

tivity with Nanoscale Morphology and Counterion Volume. *ACS Macro Letters* **2017**, *6*, 941–946.

(29) Choi, U. H.; Mittal, A.; Price, T. L.; Gibson, H. W.; Runt, J.; Colby, R. H. Polymerized Ionic Liquids with Enhanced Static Dielectric Constants. *Macromolecules* **2013**, *46*, 1175–1186.

(30) Sangoro, J. R.; Iacob, C.; Agapov, A. L.; Wang, Y.; Berdzinski, S.; Rexhausen, H.; Strehmel, V.; Friedrich, C.; Sokolov, A. P.; Kremer, F. Decoupling of ionic conductivity from structural dynamics in polymerized ionic liquids. *Soft Matter* **2014**, *10*, 3536–3540.

(31) Frenzel, F.; Borchert, P.; Anton, A. M.; Strehmel, V.; Kremer, F. Charge transport and glassy dynamics in polymeric ionic liquids as reflected by their inter- and intramolecular interactions. *Soft Matter* **2019**, *15*, 1605–1618.

(32) Sangoro, J. R.; Serghei, A.; Naumov, S.; Galvosas, P.; Kärger, J.; Wespe, C.; Bordusa, F.; Kremer, F. Charge transport and mass transport in imidazolium-based ionic liquids. *Physical Review E* **2008**, *77*.

(33) Rivera, A.; Brodin, A.; Pugachev, A.; Rössler, E. A. Orientational and translational dynamics in room temperature ionic liquids. *The Journal of Chemical Physics* **2007**, *126*, 114503.

(34) Iacob, C.; Sangoro, J. R.; Serghei, A.; Naumov, S.; Korth, Y.; Kärger, J.; Friedrich, C.; Kremer, F. Charge transport and glassy dynamics in imidazole-based liquids. *The Journal of Chemical Physics* **2008**, *129*, 234511.

(35) Sangoro, J.; Iacob, C.; Serghei, A.; Naumov, S.; Galvosas, P.; Kärger, J.; Wespe, C.; Bordusa, F.; Stoppa, A.; Hunger, J.; Buchner, R.; Kremer, F. Electrical conductivity and translational diffusion in the 1-butyl-3-methylimidazolium tetrafluoroborate ionic liquid. *The Journal of Chemical Physics* **2008**, *128*, 214509.

(36) Lee, M.; Choi, U. H.; Colby, R. H.; Gibson, H. W. Ion Conduction in Imidazolium Acrylate Ionic Liquids and their Polymers. *Chemistry of Materials* **2010**, *22*, 5814–5822.

(37) Choi, U. H.; Lee, M.; Wang, S.; Liu, W.; Winey, K. I.; Gibson, H. W.; Colby, R. H. Ionic Conduction and Dielectric Response of Poly(imidazolium acrylate) Ionomers. *Macromolecules* **2012**, *45*, 3974–3985.

(38) Choi, U. H.; Ye, Y.; de la Cruz, D. S.; Liu, W.; Winey, K. I.; Elabd, Y. A.; Runt, J.; Colby, R. H. Dielectric and Viscoelastic Responses of Imidazolium-Based Ionomers with Different Counterions and Side Chain Lengths. *Macromolecules* **2014**, *47*, 777–790.

(39) Cosby, T.; Vicars, Z.; Wang, Y.; Sangoro, J. Dynamic-Mechanical and Dielectric Evidence of Long-Lived Mesoscale Organization in Ionic Liquids. *The Journal of Physical Chemistry Letters* **2017**, *8*, 3544–3548.

(40) Frenzel, F.; Folikumah, M. Y.; Schulz, M.; Anton, A. M.; Binder, W. H.; Kremer, F. Molecular Dynamics and Charge Transport in Polymeric Polyisobutylene-Based Ionic Liquids. *Macromolecules* **2016**, *49*, 2868–2875.

(41) Põhako-Esko, K.; Taaber, T.; Saal, K.; Lõhmus, R.; Kink, I.; Mäeorg, U. New Method for Synthesis of Methacrylate-Type Polymerizable Ionic Liquids. *Synthetic Communications* **2013**, *43*, 2846–2852.

(42) Shaplov, A. S.; Lozinskaya, E. I.; Ponkratov, D. O.; Malyshkina, I. A.; Vidal, F.; Aubert, P.-H.; Okatova, O. V.; Pavlov, G. M.; Komarova, L. I.; Wandrey, C.; Vygodskii, Y. S. Bis(trifluoromethylsulfonyl)amide based "polymeric ionic liquids": Synthesis, purification and peculiarities of structure-properties relationships. *Electrochimica Acta* **2011**, *57*, 74–90.

(43) Kammakakam, I.; Bara, J. E.; Jackson, E. M.; Lertxundi, J.; Mecerreyes, D.; Tomé, L. C. Tailored CO2-Philic Anionic Poly(ionic liquid) Composite Membranes:

Synthesis, Characterization, and Gas Transport Properties. *ACS Sustainable Chemistry & Engineering* **2020**, *8*, 5954–5965.

(44) Klein, R. J.; Zhang, S.; Dou, S.; Jones, B. H.; Colby, R. H.; Runt, J. Modeling electrode polarization in dielectric spectroscopy: Ion mobility and mobile ion concentration of single-ion polymer electrolytes. *The Journal of Chemical Physics* **2006**, *124*, 144903.

(45) Serghei, A.; Tress, M.; Sangoro, J. R.; Kremer, F. Electrode polarization and charge transport at solid interfaces. *Physical Review B* **2009**, *80*.

(46) Jain, H. Composition dependence of frequency power law of ionic conductivity of glasses. *Solid State Ionics* **1998**, *105*, 129–137.

(47) Watanabe, M.; Sanui, K.; Ogata, N.; Kobayashi, T.; Ohtaki, Z. Ionic conductivity and mobility in network polymers from poly(propylene oxide) containing lithium perchlorate. *Journal of Applied Physics* **1985**, *57*, 123–128.

(48) Böhmer, R.; Ngai, K. L.; Angell, C. A.; Plazek, D. J. Nonexponential relaxations in strong and fragile glass formers. *The Journal of Chemical Physics* **1993**, *99*, 4201–4209.

(49) Angell, C.; Borick, S. Specific heats Cp, Cv, Cconf and energy landscapes of glassforming liquids. *Journal of Non-Crystalline Solids* **2002**, *307-310*, 393–406.

(50) Fragiadakis, D.; Dou, S.; Colby, R. H.; Runt, J. Molecular mobility and Li+ conduction in polyester copolymer ionomers based on poly(ethylene oxide). *The Journal of Chemical Physics* **2009**, *130*, 064907.

(51) Rivera, A.; Rössler, E. A. Evidence of secondary relaxations in the dielectric spectra of ionic liquids. *Physical Review B* **2006**, *73*.

(52) Hunger, J.; Stoppa, A.; Schrödle, S.; Hefter, G.; Buchner, R. Temperature Dependence of the Dielectric Properties and Dynamics of Ionic Liquids. *ChemPhysChem* **2009**, *10*, 723–733.

(53) Krause, C.; Sangoro, J. R.; Iacob, C.; Kremer, F. Charge Transport and Dipolar Relaxations in Imidazolium-Based Ionic Liquids. *The Journal of Physical Chemistry B* **2010**, *114*, 382–386.

(54) Fragiadakis, D.; Dou, S.; Colby, R. H.; Runt, J. Molecular Mobility, Ion Mobility, and Mobile Ion Concentration in Poly(ethylene oxide)-Based Polyurethane Ionomers. *Macromolecules* **2008**, *41*, 5723–5728.

(55) van Turnhout, J.; Wübbenhorst, M. Analysis of complex dielectric spectra. II: Evaluation of the activation energy landscape by differential sampling. *Journal of Non-Crystalline Solids* **2002**, *305*, 50–58.

(56) Wübbenhorst, M.; van Turnhout, J. Analysis of complex dielectric spectra. I. One-dimensional derivative techniques and three-dimensional modelling. *Journal of Non-Crystalline Solids* **2002**, *305*, 40–49.

(57) Díaz-Calleja, R. Comment on the Maximum in the Loss Permittivity for the Havriliak-Negami Equation. *Macromolecules* **2000**, *33*, 8924–8924.

(58) Boersma, A.; van Turnhout, J.; Wübbenhorst, M. Dielectric Characterization of a Thermotropic Liquid Crystalline Copolyesteramide: 1. Relaxation Peak Assignment. *Macromolecules* **1998**, *31*, 7453–7460.

(59) Wang, J.-H. H.; Yang, C. H.-C.; Masser, H.; Shiau, H.-S.; O'Reilly, M. V.; Winey, K. I.; Runt, J.; Painter, P. C.; Colby, R. H. Ion States and Transport in Styrenesulfonate Methacrylic PEO9 Random Copolymer Ionomers. *Macromolecules* **2015**, *48*, 7273–7285.

(60) Angell, C. A. Dynamic processes in ionic glasses. *Chemical Reviews* **1990**, *90*, 523–542.

(61) Hiemenz, P. C.; Lodge, T. P. *Polymer Chemistry*; CRC Press, 2007.

(62) Daguenet, C.; Dyson, P. J.; Krossing, I.; Oleinikova, A.; Slattery, J.; Wakai, C.; Weingärtner, H. Dielectric Response of Imidazolium-Based Room-Temperature Ionic Liquids. *The Journal of Physical Chemistry B* **2006**, *110*, 12682–12688.

(63) Chihiro Wakai, M. O., Alla Oleinikova; Weingartner, H. How Polar Are Ionic Liquids? Determination of the Static Dielectric Constant of an Imidazolium-based Ionic Liquid by Microwave Dielectric Spectroscopy. *The Journal of Physical Chemistry B* **2005**, *109*, 17028.

(64) Tudryn, G. J.; Liu, W.; Wang, S.-W.; Colby, R. H. Counterion Dynamics in Polyester-Sulfonate Ionomers with Ionic Liquid Counterions. *Macromolecules* **2011**, *44*, 3572–3582.

(65) Wang, S.-W.; Liu, W.; Colby, R. H. Counterion Dynamics in Polyurethane-Carboxylate Ionomers with Ionic Liquid Counterions. *Chemistry of Materials* **2011**, *23*, 1862–1873.

(66) Sun, T. L.; Kurokawa, T.; Kuroda, S.; Ihsan, A. B.; Akasaki, T.; Sato, K.; Haque, M. A.; Nakajima, T.; Gong, J. P. Physical hydrogels composed of polyampholytes demonstrate high toughness and viscoelasticity. *Nature Materials* **2013**, *12*, 932–937.

(67) Gordon, J. M.; Rouse, G. B.; Gibbs, J. H.; Risen, W. M. The composition dependence of glass transition properties. *The Journal of Chemical Physics* **1977**, *66*, 4971–4976.

(68) Mogurampelly, S.; Keith, J. R.; Ganesan, V. Mechanisms Underlying Ion Transport in Polymerized Ionic Liquids. *Journal of the American Chemical Society* **2017**, *139*, 9511–9514.

(69) Onsager, L. Electric Moments of Molecules in Liquids. *Journal of the American Chemical Society* **1936**, *58*, 1486–1493.

(70) Suzuki, Y.; Tsujimura, T.; Funamoto, K.; Matsumoto, A. Relaxation behavior of ran-

dom copolymers containing rigid fumarate and flexible acrylate segments by dynamic mechanical analysis. *Polymer Journal* **2019**, *51*, 1163–1172.

(71) Sasabe, H.; Saito, S. Dielectric relaxations and electrical conductivities of poly(alkyl methacrylates) under high pressure. *Journal of Polymer Science Part A-2: Polymer Physics* **1968**, *6*, 1401–1418.

(72) Wang, J.-H. H.; Colby, R. H. Exploring the role of ion solvation in ethylene oxide based single-ion conducting polyanions and polycations. *Soft Matter* **2013**, *9*, 10275.

(73) Macdonald, J. R. Theory of ac Space-Charge Polarization Effects in Photoconductors, Semiconductors, and Electrolytes. *Physical Review* **1953**, *92*, 4–17.

(74) Coelho, R. Sur la relaxation d'une charge d'espace. *Revue de Physique Appliquée* **1983**, *18*, 137–146.